

Electron collisions with boron trichloride (BCl_3) molecules

Alicja Domaracka, Elżbieta Ptasńska-Denga, and Czesław Szmytkowski*

*Atomic Physics Group, Faculty of Applied Physics and Mathematics, Gdańsk University of Technology,
ul. G. Narutowicza 11/12, 80-952 Gdańsk, Poland*

(Received 24 February 2005; published 25 May 2005)

Absolute total cross section (TCS) for electron scattering by boron trichloride (BCl_3) molecules has been measured in a linear transmission method under single collision conditions. Measurements have been performed within electron energy range from 0.3 to 370 eV. The TCS energy function for BCl_3 is dominated with very pronounced enhancement peaked near 10 eV ($61 \times 10^{-20} \text{ m}^2$ in the maximum). Low-energy slope of the enhancement is superimposed with two resonantlike structures located near 3.2 and 6.0 eV. On the descending high-energy side of the TCS curve only a weak shoulder between 30 and 60 eV is discernible. The present TCS is compared with the existing experimental and calculated cross sections for particular e^- - BCl_3 scattering processes. Furthermore, the TCS for BCl_3 is also confronted with the TCS for BF_3 and the role of peripheral atoms in molecule is indicated and discussed.

DOI: 10.1103/PhysRevA.71.052711

PACS number(s): 34.80.Bm, 34.80.Gs

I. INTRODUCTION

Boron trichloride is extensively used in the industrial applications to materials processing (plasma-enhanced etching [1], deposition and/or doping of boron [2]) and in organic synthesis [3]. For thorough understanding, modeling and controlling undergoing phenomena in plasma processing mixtures containing BCl_3 , comprehensive sets of reliable cross sections and reaction rates for processes involving BCl_3 and its fragments in the ground and excited states are needed. Despite such importance of BCl_3 for present-day technologies, availability of basic data for electron-induced processes in this compound is still very poor. The deficiency of absolute experimental data on e^- - BCl_3 scattering is mainly connected with physicochemical properties of BCl_3 gas. By the reason of its high reactivity and corrosiveness, scattering experiments with BCl_3 —especially those with the use of crossed-beam techniques—are difficult to handle and the obtained results have serious uncertainties [4].

The early experimental studies of BCl_3 molecules involved electrons as projectile concerned electron diffraction [5]. Later, investigations focused mainly on the electron-induced formation of positive [6–11] and negative ions [8,10–15] using electron-beam and swarm techniques. Those experiments provided information on appearance potentials and/or gave only relative abundances of the observed ions. Absolute experimental cross-section data are fragmentary, and are available for the electron attachment to the BCl_3 molecule [12,15], partial and total electron-induced ionization [11], and for the emission from excited molecular fragments produced by electron impact [16–18]. Vibrational and dissociation (into neutral fragments) cross sections have been derived [19] from experimental electron drift velocities [20]. Furthermore, in the literature one can also find the threshold electron-impact excitation spectra [13] of BCl_3 molecules and the electron transmission spectra [21]. Most of the quan-

titative data on the electron- BCl_3 scattering have been derived from swarm experiments.

The lack of experimental data on elastic e^- - BCl_3 scattering has been to some degree filled in with calculated elastic cross sections obtained using different theoretical formalisms [21–25]. Comparison shows that results of those calculations distinctly depend on the approach applied. Also available are calculations of the total cross section for the dissociation of BCl_3 by electron impact [22]. Further, model calculations are employed [26–28] to extend low-intermediate experimental ionization data [11] to higher energies.

Motivated by the scarcity of absolute e^- - BCl_3 scattering data as a function of electron energy, we have performed an experiment in which the absolute total cross section (TCS) for the BCl_3 molecule has been determined over a wide energy range, from low to intermediates (0.3–370 eV). The TCS results provide some test of the reliability of theoretical models and computational procedures used in elastic calculations. They may also serve as an upper limit reference for future studies on e^- - BCl_3 scattering. To get a better understanding of how peripheral atoms influence the electron scattering we have made a comparison of the present TCS data for BCl_3 with our recent measurements for BF_3 molecule. Some similarities and differences are pointed out.

II. EXPERIMENTAL PROCEDURE

The present total e^- - BCl_3 scattering cross section has been measured using the electron transmission method [29] in a linear configuration. This method relates the TCS to the transparency of the gas target for a beam of electrons; higher transparency responds to lower TCS. The apparatus and measuring procedure used in the present experiment are essentially the same as described in detail elsewhere [30,31]. The electron beam is formed by an electron optics system which comprises an electron gun followed by an energy dispersing 127° cylindrical electrostatic monochromator, and a zoom lens system. Electrons of a given energy E , with an energy spread of 80–100 meV (full width at half maximum), are

*Electronic address: czsz@mif.pg.gda.pl

injected into a scattering chamber. The electrons which pass the scattering volume are energy discriminated by a retarding-field element and eventually detected by a Faraday cup. When target molecules are admitted into the scattering cell, the transmitted electrons suffer scattering which reflects in the attenuation of a detected electron current.

The quantities taken in the present experiment are: $I(p, E)$ and $I(p=0, E)$ —the intensities of the transmitted currents of electrons of given energy E in the presence and absence of the target gas in the scattering cell, respectively, p —the pressure of the investigated target gas in the scattering cell, T_c —the temperature of the scattering cell, and T_m —the temperature of the mks manometer head (322 K). To determine the TCS value, $Q(E)$, we used the Bouguer-de Beer-Lambert (BBL) attenuation formula:

$$I(p, E) = I(p=0, E) \exp\left(-\frac{pl}{kT_g} Q(E)\right),$$

where l is the effective path length of electrons in the target volume, $T_g = \sqrt{T_m T_c}$ is the effective temperature of the target gas when the thermal transpiration effect [32] is accounted for, and k is the Boltzmann constant. As all required quantities are directly measured or evaluated, the resulting TCS values are absolute. The energy scale of the incident electrons was defined by the voltage applied to a lens element and the energy calibration against the well-known standard—the 2.3-eV resonant oscillatory structure in N_2 . The uncertainty of the energy scale is about 0.1 eV; half of this value is related to the shift in the contact potentials observed in the course of experiment.

Before the TCS measurements commenced, the electron optics and gas supplying system were carefully processed to remove traces of moisture from surfaces what reduces hydrolysis of BCl_3 . Next, the electron optics was passivated in the presence of BCl_3 until the electron transmission becomes stabilized enough to start measurements. It is worth noting that the pressure of the sample in the scattering cell in the course of the experiment was kept at the level two to three times lower than in our previous measurements. Such a procedure ensured stable filament emission and the intensity of the primary electron current throughout the experiment.

At each selected electron energy, individual cross-section measurements were carried out over a range of the electron optics and the target pressure conditions. The results from different series obtained at a given energy appeared to be independent (within limits of statistical uncertainties) of applied sample pressures (20–80 mPa) and the intensity of the incident electron beam (0.2–100 pA). The final value of the TCS at each particular energy is an average of a number of data obtained in series (3–13) of individual runs (6–10 in a series). The scatter of TCS results (one standard deviation of the weighted mean value) reaches about 2–3 % below 2 eV, gradually decreases to 1–2 % between 2 and 4 eV and to less than 1% within 5–200 eV, and finally increases to 1.5% at higher energies used.

There is a number of unavoidable effects which may significantly change the measured TCS. Two of them are inherently related to the electron transmission method applied.

The first one, which systematically lowers the obtained TCS values, is associated with the imperfect discrimination by the detector system of electrons scattered into small forward angles. Based on calculated angular distributions of 0.2–40-eV electrons scattered elastically [23,24] we estimated that the extent to which the forwardly scattered low-energy electrons could lower the measured TCS in the present experiment is well underneath 0.5%. At high impact energies, where forward scattering markedly increases, no differential cross sections are available as yet. However, estimations made for other nonpolar targets suggest that at the highest energies applied the lessening of TCS should not exceed 2% for the present geometry of the electron collector. The second factor affecting the measured TCS is connected with the end effects at the entrance and exit apertures of the scattering cell. The target gas flowing through the chamber orifices does not allow us to determine accurately the real path length of electrons within the target of inhomogeneous density; to be more precise, the resulting uncertainty comprises the whole numerator pl , in the BBL formula. The uncertainty related to that factor was estimated to be lower than 2.5% (cf. Ref. [33]).

In addition to the aforementioned, there are two extra effects associated with properties of BCl_3 molecule which may alter the measured TCS values. The first one is related to high hydrolycity of BCl_3 molecule leading to possible presence of HCl in the sample. Because the TCS for HCl is relatively high at low energies and tends to increase towards zero energy (from $26 \times 10^{-20} \text{ m}^2$ at 2 eV to $43 \times 10^{-20} \text{ m}^2$ around 0.8 eV [34]), the presence of HCl may distinctly enlarge the measured TCS at the lowest energies used. On the other hand, above 2 eV, where TCS for BCl_3 becomes to be higher than that for HCl, the presence of HCl can lower the measured TCS for BCl_3 . We believe, however, that this factor does not exceed the statistical scatter of results because the measured TCS was independent of whether the sample gas was injected into scattering volume directly from the cylinder or from the auxiliary storage-gas reservoir. A commercially supplied sample of BCl_3 from Aldrich with a stated purity of 99.9% was used without further purification and no analysis of the gas in the scattering cell was made. The other effect which contributes to the TCS uncertainty is related to the influence of the BCl_3 molecules on the electron optics elements which, in consequence, shifts the energy scale in the course of the experiment. This effect leads to broadening and flattening of sharp features in the TCS energy function; resulting uncertainties in the present experiment may be especially troublesome below 6 eV where they amount to 2–4 %.

The overall systematic uncertainty in the measured TCS is estimated as a quadrature sum of all possible systematic errors encountered in the measurements of individual quantities used for the derivation of the TCS. Below 4 eV it is about 5–6 %, decreasing gradually to 3% between 5 and 150 eV, and increasing again to 4% at the highest applied energies.

III. RESULTS AND DISCUSSION

A. Boron trichloride, BCl_3

Figure 1 shows the variation of our absolute total electron-scattering cross section for the BCl_3 molecule with

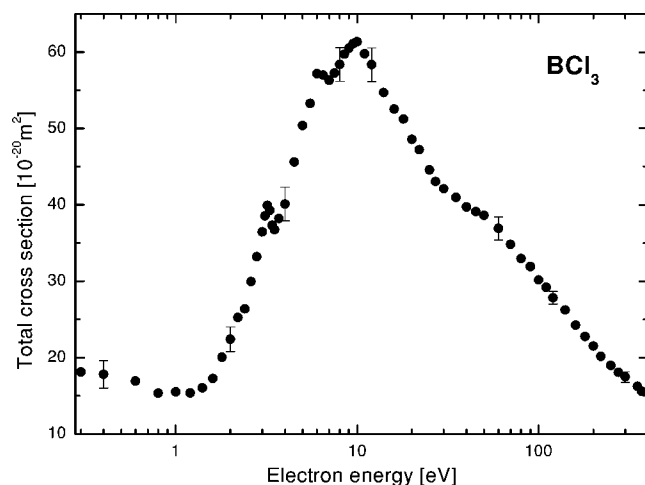


FIG. 1. Present experimental total absolute cross section for e^- - BCl_3 scattering; error bars represent overall (systematic plus statistical) uncertainties.

an incident electron energy. Results have been obtained in the linear electron transmission experiment over the energy range from 0.3 to 370 eV. In Table I the numerical TCS values from the present experiment are listed.

The most striking feature of the measured TCS in the investigated energy range is a broad, very distinct enhancement with the maximum ($61 \times 10^{-20} \text{ m}^2$) located near 10 eV. On the low-energy slope of the enhancement two weak fea-

TABLE I. Absolute electron-scattering total cross sections for BCl_3 molecules in 10^{-20} m^2 .

E (eV)	TCS	E (eV)	TCS	E (eV)	TCS
0.3	18.1	4.5	45.6	35	41.0
0.4	17.8	5.0	50.4	40	39.7
0.6	16.9	5.5	53.3	45	39.1
0.8	15.3	6.0	57.2	50	38.6
1.0	15.5	6.5	57.0	60	36.9
1.2	15.3	7.0	56.3	70	34.8
1.4	16.0	7.5	57.2	80	33.0
1.6	17.2	8.0	58.4	90	31.9
1.8	20.0	8.5	59.7	100	30.2
2.0	22.4	9.0	60.5	110	29.2
2.2	25.2	9.5	61.1	120	27.8
2.4	26.4	10	61.4	140	26.2
2.6	30.0	11	59.8	160	24.2
2.8	33.2	12	58.4	180	22.8
3.0	36.4	14	54.7	200	21.5
3.1	38.5	16	52.5	220	20.2
3.2	39.9	18	51.2	250	19.0
3.3	39.3	20	48.6	275	18.0
3.4	37.3	22	47.2	300	17.4
3.5	36.7	25	44.6	350	16.2
3.7	38.2	27	43.0	370	15.6
4.0	40.1	30	42.1		

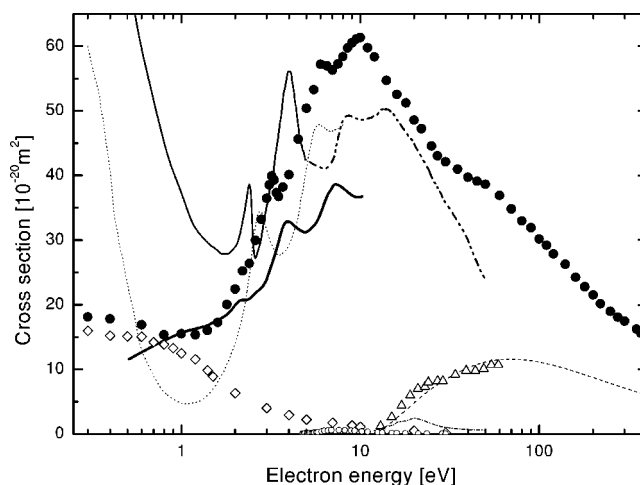


FIG. 2. Comparison of the present total e^- - BCl_3 cross section (full circles) with some partial cross sections. To keep the figure more legible we show only selected data; for more comprehensive synthesis of data the reader is addressed to Ref. [4]. Experimental: open diamonds, vibrational [19]; open triangles, ionization [11]; open circles, dissociation [19]. Theoretical: full line, integral elastic, static-exchange (SE) potential [21]; thick dashed-dot-dot line, integral elastic, SE potential [24]; thick full line, integral elastic, static-exchange-polarization (SEP) potential [22], data read out from Ref. [4]; dotted line, integral elastic, SEP potential [23]; dashed-dot line, dissociation [22]; data read out from Ref. [4]; dashed line, ionization, binary-encounter-Bethe (BEB) approximation [27].

tures are superimposed: the first peak is more pronounced, and spans between 2.6 and 3.5 eV with the maximum ($40 \times 10^{-20} \text{ m}^2$) at 3.2 eV, while the second one, less marked, peaks around 6 eV ($57 \times 10^{-20} \text{ m}^2$). Beyond 10 eV the TCS energy function decreases with the energy increase. Up to 30 eV the TCS decreases quite steeply. From 30 eV the slope of the TCS curve distinctly changes and a weak shoulder is discernible between 30 and 60 eV. Above 60 eV the decline increases again and the behavior of the TCS energy function can be described with the regression formula $Q(E) \sim E^{-a}$, where $a = 0.45 \pm 0.1$. Such an energy dependence means that the intermediate-energy TCS is nearly proportional to the time the incoming electron needs to pass the distance equal to dimension of the target molecule. At the highest energy used, 370 eV, the TCS falls to nearly $16 \times 10^{-20} \text{ m}^2$, the value which rather accidentally coincides with the low-energy TCS around the minimum visible close to 1 eV.

As no total e^- - BCl_3 cross section is available in the literature to compare with the present results, in Fig. 2 we have shown our TCS together with experimental cross sections for particular electron-induced processes leading to vibrational excitation [19], dissociation [19], and to ionization [11] of BCl_3 molecule. Calculated cross sections for elastic scattering [21–24], dissociation [22], and for ionization [27] are also presented. Figure 2 clearly shows that explicit explanation of the TCS behavior below 1 eV, based on those data, is a rather difficult task. The magnitude of the summed cross section for electron impact excitation of BCl_3 vibrational levels ($n=1+2, 3$, and 4) [19] may suggest that the vibrational excitation contributes essentially to TCS below 1 eV; note

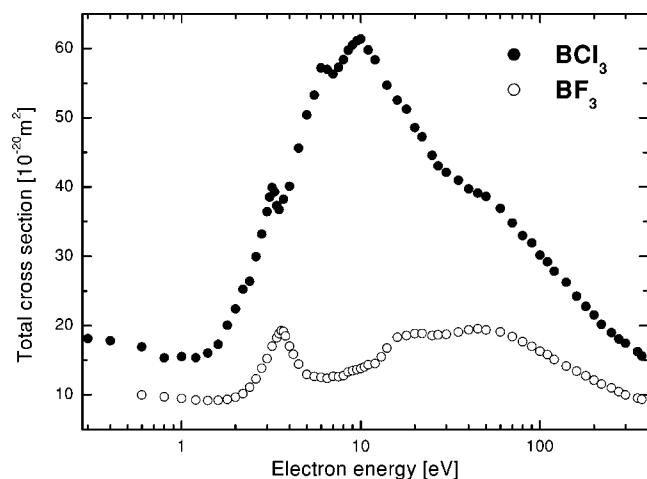


FIG. 3. Illustration of the role of peripheral atoms in the electron scattering. Experimental total cross sections: full circles, BCl_3 , present; open circles, BF_3 [35].

also that the shape of this “total” vibrational cross section is below 1 eV very similar to the TCS curve. Critical analysis of the procedure used in the determination of that cross section indicate, however, that the magnitude of the vibrational data might be distinctly overestimated (see Ref. [4]). On the other hand, the integral cross sections calculated by different groups differ to such an extent that no definite conclusions could be drawn onto the role of elastic scattering at very low energies. While elastic calculations of McKoy *et al.* [22] monotonously decrease below 1 eV in reasonable accord with the present TCS, the results of Tossell *et al.* [21] and Isaacs *et al.* [23] below 1 eV rapidly increase as the energy approaches zero. Dissociative electron attachment, which seems to be a leading scattering channel at near-zero energies [15], between 0.3 and 1 eV contributes a little to electron scattering [12].

Calculations [21–24] clearly show that the increase of the TCS beyond the 1-eV minimum ($16 \times 10^{-20} \text{ m}^2$) must be essentially associated with elastic processes. Along with the pronounced broad background related to direct scattering, the calculations also revealed some distinct resonant structures located below 10 eV. These structures were attributed to formation of temporary negative-ion states when the impinging electron attaches to the target molecule. The resonant peaks in calculated cross sections are placed, however, at energies that differ from those visible in the present experimental TCS, and the difference depends on the potential used in calculations. In the experiment, the resonant structures were noticed near 2.5 and 8 eV by Stockdale *et al.* [13] in the threshold electron impact excitation spectrum and at 2.86, 5.16, 7.57, and 9.05 eV by Tossell *et al.* [21] in their derivative transmission spectra. The location of the 2.86-eV feature corresponds to our 3.2-eV TCS maximum, while the 5.2- and 7.6-eV features are situated within the region of our 6.0-eV structure. It is worth noting that the structures located between 5 and 8 eV and 10 eV were also observed in TCSs for other perchlorinated molecules (CCl_4 , SiCl_4 , and GeCl_4) [30] and therefore we believe the 6.0- and 10-eV features visible in the TCS for BCl_3 are characteristic for targets with

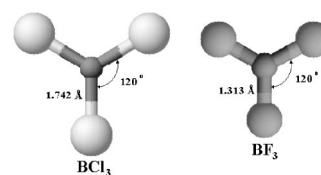


FIG. 4. Schematic of the BCl_3 and BF_3 geometry.

peripheral chlorine atoms. Integral cross sections calculated in static-exchange approximation for metal trichlorides (BCl_3 , AlCl_3 , and GaCl_3) clearly display the presence of resonant structure at around 8 eV [25]; it could be shifted towards lower energy by about 1–2 eV, in better agreement with our TCS, if more realistic potential is used. A similar shift in the energy of the maximum was also observed in the calculated cross section for the BF_3 molecule [25].

Beyond the main TCS maximum at 10 eV the role of elastic scattering still remains essential, although above the threshold the contribution of electron-induced ionization processes constantly increases. The weak shoulder spanned between 30 and 60 eV may just reflect the significant increase of ionization efficiency with the maximum around 60–70 eV.

B. Comparison of TCSs for BCl_3 and BF_3

To examine how external atoms in a molecule affect the electron-scattering cross sections we compared the present TCS for e^- - BCl_3 scattering with our measurements for BF_3 (Fig. 3) [35].

The neutral boron halides BCl_3 and BF_3 are “closed shell” planar and symmetric (D_{3h}) molecules (see Fig. 4), both are nonpolar. Therefore one would expect some similarities in the shape of their electron impact cross sections. Earlier results [30], however, indicate the lack of any similarities in the shape of TCSs for the other perfluorinated targets and their perchlorinated counterparts. From Fig. 3 it is clearly evident that the substitution of chlorine atoms for fluorine in the target molecule changes drastically the magnitude and shape of the TCS over the whole energy range studied. According to the shape of TCSs for BCl_3 and BF_3 , the only similarities worth attention are visible below 3 and 4 eV. Especially interesting is that both compared TCSs have their resonant maximum located around similar energy: close to 3.6 eV for BF_3 and near 3.2 eV for BCl_3 . Such similarity may suggest that both resonances are mostly associated with the central boron atom.

Regarding the magnitude, over the entire energy range investigated the TCS for BCl_3 is significantly higher than

TABLE II. Molecular ionization potentials IP, bond lengths B–X ($X=\text{Cl}, \text{F}$), the gas-kinetic cross sections σ , and electric dipole polarizabilities α ; data are from Ref. [36].

Molecule	IP (eV)	B–X (10^{-10} m)	σ (10^{-20} m^2)	α (10^{-30} m^3)
BCl_3	11.60	1.742	16.6	9.38
BF_3	15.56	1.313	9.66	3.31

that for BF_3 . This difference only in part may be explained in terms of the larger geometrical size of a chlorine containing molecule. That is, a case in the vicinity of 1 eV and around 300 eV where the ratio of TCSs for BCl_3 and BF_3 is about 1.7 and equals the proportion of their geometrical dimensions as well as their gas-kinetic cross sections (see Table II). In the remaining energy range, differences significantly exceed those resulting from the molecular geometry and become particularly striking between 4 and 60 eV where TCSs for BF_3 and BCl_3 behave quite differently. One of the reasons for such great difference is that the TCS for BF_3 has the minimum in the energy range where the TCS for BCl_3 has its maximum. Such behavior is characteristic for all perfluorides studied so far; the TCS for perfluorinated targets has the minimum located between 6 and 20 eV (cf. Refs. [35,37]) and around 10 eV is even smaller than that for perhydrides—molecules of smaller size. On the other hand, the prominent magnitude of TCS for BCl_3 around 10 eV must be related to distinctly higher electric polarizability of the molecule (Table II). Due to lack of static dipole field, the long-range polarization potential becomes the important component of electron-molecule interaction. The same holds also for other molecules with peripheral chlorine atoms.

IV. SUMMARY

We presented the absolute total electron-scattering cross section for BCl_3 molecule measured in a linear transmission

experiment from 0.3 to 370 eV. The TCS energy dependence for BCl_3 shows one very distinct enhancement peaked near 10 eV. This enhancement is superimposed with resonant features located at 3.2, 6, and 10 eV. The 6- and 10-eV structures seem to be characteristic for perchlorinated targets. On the high-energy slope of the TCS curve a broad shoulder spans between 30 and 60 eV. From the comparison of the TCS data with available experimental and theoretical results for particular electron impact processes it is clear that the current level of understanding e^- - BCl_3 scattering is still not satisfactory and to explain all observed features of TCS for BCl_3 and quantify the scattering process more detailed experimental studies, especially those with the use of high-resolution crossed-beam techniques in various scattering channels, are required. A comparison of the TCS for BCl_3 with that for BF_3 indicates an essential role of the external atoms in the electron-scattering process.

ACKNOWLEDGMENTS

The authors acknowledge partial support from the Polish Ministry of Education (MENiS) and Ministry for Research and Informatization (MNiI).

-
- [1] B. J. Howard and Ch. Steinbrüchel, *J. Vac. Sci. Technol. A* **12**, 1259 (1994); I-S. Jin, H-H. Park, K-H. Kwon, and C-I. Kim, *Microelectron. Eng.* **33**, 223 (1997).
 - [2] R. B. Jackman, B. Baral, C. R. Kingsley, and J. S. Foord, *Diamond Relat. Mater.* **5**, 378 (1996).
 - [3] G. W. Kabalka and Z. Wu, *Tetrahedron Lett.* **41**, 579 (2000).
 - [4] L. G. Christophorou and J. K. Olthoff, in *Fundamental Electron Interactions with Plasma Processing Gases* (Kluwer/Plenum, New York, 2004).
 - [5] R. Wierl, *Ann. Phys.* **8**, 521 (1931); A. H. Gregg, G. C. Hampson, G. I. Jenkins, P. L. F. Jones, and L. E. Sutton, *Trans. Faraday Soc.* **33**, 852 (1937); H. A. Lévy and L. O. Brockway, *J. Am. Chem. Soc.* **59**, 2083 (1937).
 - [6] O. Osberghaus, *Z. Phys.* **128**, 366 (1950).
 - [7] R. W. Law and J. L. Margrave, *J. Chem. Phys.* **25**, 1086 (1956).
 - [8] J. Marriott and J. G. Craggs, *J. Electron. Control* **3**, 194 (1957).
 - [9] W. S. Koski, J. J. Kaufman, and C. F. Pachucki, *J. Am. Chem. Soc.* **81**, 1326 (1959).
 - [10] L. J. Overzet and L. Luo, *Appl. Phys. Lett.* **59**, 161 (1991).
 - [11] C. Q. Jiao, R. Nagpal, and P. Haaland, *Chem. Phys. Lett.* **265**, 239 (1997).
 - [12] N. S. Buchel'nikova, *Zh. Eksp. Teor. Fiz.* **35**, 1119 (1958); [*Sov. Phys. JETP* **35**, 783 (1959)]; *Fortschr. Phys.* **8**, 626 (1960).
 - [13] J. A. Stockdale, D. R. Nelson, F. J. Davis, and R. N. Compton, *J. Chem. Phys.* **56**, 3336 (1972).
 - [14] Z. Lj. Petrović, W. C. Wang, M. Suto, J. C. Han, and L. C. Lee, *J. Appl. Phys.* **67**, 675 (1990).
 - [15] C. Tav, P. G. Datskos, and L. A. Pinnaduwaage, *J. Appl. Phys.* **84**, 5805 (1998).
 - [16] Z. J. Jabbour, K. E. Martus, and K. Becker, *J. Phys. D* **9**, 263 (1988).
 - [17] P. G. Gilbert, R. B. Siegel, and K. Becker, *Phys. Rev. A* **41**, 5594 (1990).
 - [18] I. Tokue, M. Kudo, M. Kusakabe, T. Honda, and Y. Ito, *J. Chem. Phys.* **96**, 8889 (1992).
 - [19] R. Nagpal and A. Garscadden, *Appl. Phys. Lett.* **64**, 1626 (1994).
 - [20] D. L. Mosteller, Jr., M. L. Andrews, J. D. Clark, and A. Garscadden, *J. Appl. Phys.* **74**, 2247 (1993).
 - [21] J. A. Tossell, J. H. Moore, and J. K. Olthoff, *Int. J. Quantum Chem.* **XXIX**, 1117 (1986).
 - [22] V. McKoy, C. Winstead, and W. L. Morgan, in *Data Compilation for Plasma Chemistries*, Technology Transfer No. 97043274A-TR, SEMATECH, August 22, 1997.
 - [23] W. A. Isaacs, C. W. McCurdy, and T. N. Rescigno, *Phys. Rev. A* **58**, 2881 (1998).
 - [24] M. H. F. Bettega, *Phys. Rev. A* **61**, 042703 (2000); **62**, 024701 (2000).
 - [25] R. F. da Costa, L. G. Ferreira, M. A. P. Lima, and M. H. F. Bettega, *J. Chem. Phys.* **118**, 75 (2003).
 - [26] H. Deutsch, K. Becker, and T. D. Märk, *Int. J. Mass Spectrom. Ion Processes* **167/168**, 503 (1997).
 - [27] Y.-K. Kim and K. K. Irikura, in *Atomic and Molecular Data and Their Applications* (AIP, Melville, NY, 2000), p. 220.
 - [28] M. Probst, H. Deutsch, K. Becker, and T. D. Märk, *Int. J.*

- Mass. Spectrom. **206**, 13 (2001).
- [29] B. Bederson and L. J. Kieffer, Rev. Mod. Phys. **43**, 601 (1971).
- [30] Cz. Szmytkowski, P. Możejko, and G. Kasperski, J. Phys. B **31**, 3917 (1998).
- [31] Cz. Szmytkowski and P. Możejko, Vacuum **63**, 549 (2001).
- [32] M. Knudsen, Ann. Phys. **31**, 205 (1910).
- [33] R. N. Nelson and S. O. Colgate, Phys. Rev. A **8**, 3045 (1973).
- [34] E. Brüche, Ann. Phys. **82**, 25 (1927); A. Hamada and O. Sueoka, J. Phys. B **27**, 5055 (1994).
- [35] Cz. Szmytkowski, M. Piotrowicz, A. Domaracka, Ł. Kłosowski, E. Ptasińska-Denga, and G. Kasperski, J. Chem. Phys. **121**, 1790 (2004).
- [36] In *Handbook of Chemistry and Physics*, edited by D. R. Lide, 76th edition (CRC Press, Boca Raton, 1995-1996).
- [37] Cz. Szmytkowski, A. Domaracka, P. Możejko, E. Ptasińska-Denga, Ł. Kłosowski, M. Piotrowicz, and G. Kasperski, Phys. Rev. A **70**, 032707 (2004).